Eur. Phys. J. A **29**, 281–287 (2006)
DOI 10.1140/epja/i2006-10091-y

THE EUROPEAN PHYSICAL JOURNAL A

Measurement of evaporation residue cross-sections of the reaction ^{30}Si + ^{238}U at subbarrier energies

K. Nishio[1,2,a], S. Hofmann[1,3,b], F.P. Heßberger[1], D. Ackermann[1], S. Antalic[4], V.F. Comas[5], Z. Gan[6], S. Heinz[1], J.A. Heredia[5], H. Ikezoe[2], J. Khuyagbaatar[1,7], B. Kindler[1], I. Kojouharov[1], P. Kuusiniemi[8], B. Lommel[1], R. Mann[1], M. Mazzocco[1], S. Mitsuoka[2], Y. Nagame[2], T. Ohtsuki[9], A.G. Popeko[10], S. Saro[4], H.J. Schött[1], B. Sulignano[1,11], A. Svirikhin[10], K. Tsukada[2], K. Tsuruta[2], and A.V. Yeremin[10]

[1] Gesellschaft für Schwerionenforschung mbH, D-64220 Darmstadt, Germany
[2] Japan Atomic Energy Agency, Tokai, Ibaraki 319-1195, Japan
[3] Institut für Kernphysik, Johann Wolfgang Goethe-Universität, D-60486 Frankfurt am Main, Germany
[4] Department of Nuclear Physics, Comenius University, SK-84215 Bratislava, Slovakia
[5] Higher Institue of Technologies and Applied Sciences, Habana 10400, Cuba
[6] Institute of Modern Physics, Chinese Academy of Sciences, Lanzhou 730000, PRC
[7] St. Petersburg State University, 198504 Stari Petergof, St. Petersburg, Russia
[8] CUPP, University of Oulu, FIN-86801 Pyhäjärvi, Finland
[9] Laboratory of Nuclear Science, Tohoku University, Sendai 982-0826, Japan
[10] Flerov Laboratory of Nuclear Reactions, JINR, 141 980 Dubna, Russia
[11] Institut für Kernchemie, Johannes Gutenberg-Universität Mainz, D-55099 Mainz, Germany

Received: 12 July 2006 / Revised: 25 August 2006 /
Published online: 14 September 2006 –
Communicated by R. Krücken

Abstract. The reaction $^{30}\mathrm{Si} + ^{238}\mathrm{U} \rightarrow ^{268}\mathrm{Sg}^*$ was studied at beam energies close to the Coulomb barrier. At a center-of-mass energy of $E_{\mathrm{c.m.}} = 144.0\,\mathrm{MeV}$ for reactions at half thickness of the target we measured three decay chains of ^{263}Sg produced by evaporation of five neutrons. The cross-section was (67^{+67}_{-37}) pb. At $E_{\mathrm{c.m.}} = 133.0\,\mathrm{MeV}$ we measured three spontaneously fissioning nuclei which we assigned to the isotope ^{264}Sg. The production cross-section was (10^{+10}_{-6}) pb and a half-life of (120^{+126}_{-44}) ms was determined. This half-life is a factor of twenty shorter than theoretical predictions. At $E_{\mathrm{c.m.}} = 128.0\,\mathrm{MeV}$ an upper cross-section limit of 15 pb was measured. The cross-section data reveal a strong influence of the orientation of the deformed target nucleus on the production yield. Compared to excitation functions measured for the lighter system $^{16}\mathrm{O} + ^{238}\mathrm{U} \rightarrow ^{254}\mathrm{Fm}^*$, a reduction of the fusion probability was observed at low beam energies indicating increasing competition from quasifission processes.

PACS. 25.60.Pj Fusion reactions – 23.60.+e α decay – 25.85.Ca Spontaneous fission – 27.90.+b $220 \leq A$

1 Introduction

Two types of fusion reactions which significantly differ by the amount of released thermal energy were successfully used in synthesis of heavy and superheavy elements (SHE). These are the cold-fusion reactions based on lead or bismuth targets and the hot-fusion reactions based on actinide targets. Using cold-fusion reactions isotopes of elements up to proton number 112 [1] were produced at GSI in Darmstadt, Germany, up to proton number 113 [2] at RIKEN in Wako, Japan, and using hot-fusion reactions isotopes of elements up to 116 and one isotope of element 118 [3,4] were produced at FLNR in Dubna, Russia.

Another difference between the two reactions is associated with the static deformation of the target nuclei. Experimental data from measurement of excitation functions reveal that in the case of cold-fusion highest cross-sections are obtained at beam energies where a contact configuration between the projectile and the spherical target nucleus is just reached [1]. In the case of hot fusion the cross-section maxima were measured at beam energies which are high enough so that projectile (^{48}Ca) and prolate target nuclei can come into contact at minimal distance (equatorial collisions) and thus form a most compact starting configuration on the way to the compound nucleus. The cross-sections drop rapidly when the energy is decreased to values where the interaction is limited to polar colli-

[a] e-mail: nishio.katsuhisa@jaea.go.jp
[b] Josef Buchmann-Professor Laureatus.

sions. In this case the probability for re-separation of the reaction partners is high.

However, the results are different in the case of projectiles significantly lighter than ^{48}Ca. In the reaction $^{16}\mathrm{O} + ^{238}\mathrm{U}$, *e.g.*, the experimental data show a large enhancement of evaporation residue (ER) cross-sections at sub-barrier energies [5], indicating fusion independent of the orientation of the target nucleus.

In the frame of the hypothesis given before, we expect a transition from the orientation-independent fusion using light projectiles to the case of equatorial fusion only using ^{48}Ca projectiles. In order to study the anticipated transition we used the reaction $^{30}\mathrm{Si} + ^{238}\mathrm{U}$ with a projectile right in the middle between ^{16}O and ^{48}Ca. The compound nucleus is ^{268}Sg. In the case of subbarrier fusion, we expect production of the isotope ^{264}Sg via the 4n evaporation channel. This isotope was not known until recently, when it was first observed at LBNL using the same reaction as studied here [6]. Our cross-section data are compared with results from fusion evaporation models taking into account effects of the static prolate deformation of the target nucleus on the fusion process. Similar arguments were discussed and presented in earlier work on reactions using prolately deformed target nuclei of rare-earth elements [7–10].

2 Experimental technique

The experiment was performed at the linear accelerator UNILAC and at the velocity filter SHIP of GSI in Darmstadt. The beam of $^{30}\mathrm{Si}^{6+}$ was prepared from isotopically enriched material, ^{30}SiO, enrichment 99.5%, at the High Charge State Injector (HLI) consisting of a 14 GHz ECR ion source, RFQ and IH structure accelerators. At an energy of 1.4 × A MeV the beam was injected into the Alvarez sections and accelerated up to 4.8 × A MeV. Subsequently, the fine tuning of the energy was achieved with single resonators.

Average beam intensities were typically (0.7–1.0) $p\mu$A at a pulse structure of 5.0 ms wide pulses and 50 Hz repetition frequency.

The SHIP set-up is essentially the same as in previous experiments. It consists of a rotating target wheel, the velocity filter SHIP (Separator for Heavy-Ion reaction Products), and the detector system in the focal plane. Detailed descriptions can be found in [1,11–14].

The uranium targets were prepared by evaporation of isotopically depleted $^{238}\mathrm{UF}_4$ (< 0.4 % ^{235}U) and by condensation on 45 μg/cm^2 carbon backing. The $^{238}\mathrm{UF}_4$ target layers had thicknesses of 375–404 μg/cm^2, which were coated by a 15 μg/cm^2 thick carbon layer to prevent losses of material due to sputtering. Eight targets were mounted at the rim of a wheel of 15 cm radius. The side with the thin carbon layer was mounted downstream. Four wheels were used during the experiment. The wheels rotated at a frequency of 1125 rpm synchronously to the pulse structure of the beam. The target thickness was monitored continuously using the scattering of 20 keV electrons [15] and elastically scattered projectiles. The reaction energy in the center-of-mass system at the beginning and end of the $^{238}\mathrm{UF}_4$ layer differed by +0.9 MeV and −0.9 MeV, respectively, from the reaction energy in the middle of the target thickness due to energy loss of the beam.

The efficiency of SHIP is significantly reduced by the scattering of the relatively slow ERs in the target and by the recoil momentum from the evaporation of 3–5 neutrons. Using a Monte Carlo calculation we obtained an efficiency of 11%. Due to the relatively wide distribution of the ERs in the focal plane, we lost about 10% of the ERs which passed SHIP, by the detector. Combining the uncertainties of the efficiency values, beam dose measurement, and target thickness, we estimated a 50% uncertainty of the extracted absolute cross-section values. However, the relative uncertainty between the data of an excitation function is given by the statistical fluctuation of the measured number of events.

In the focal plane of SHIP, ERs and their subsequent α decay and/or spontaneous fission (sf) are detected by a position-sensitive 16-strip Si PIPS detector. The active area of this "stop detector" is 80 mm × 35 mm. Escaping α particles or fission fragments are detected by a "box detector" which covers an area of 85% of the backward hemisphere.

A timing detector is located in front of the silicon detector array. Besides a time-of-flight energy measurement obtained together with signals from the silicon detector, it is used for distinguishing signals from implanted ERs or background particles from radioactive decay events. These veto signals are obtained from electrons which are emitted when ions are passing through a 35 μg/cm^2 carbon foil. The detector is movable. It was moved out of the particle trajectories for testing the range of the relatively slow ERs during some of the irradiations at the beginning of the experiment. In this case the radioactive decays were detected during the 15.0 ms beam-off periods.

The silicon detectors were calibrated using α-rays from ^{252}No and its decay products ^{248}Fm and ^{244}Cf, produced in the reaction $^{48}\mathrm{Ca} + ^{206}\mathrm{Pb} \rightarrow ^{254}\mathrm{No}^*$. The energy resolution for fully stopped α's was typically 25 keV (FWHM) for the 8415 keV α particles from ^{252}No. For the energy of escaping α particles detected in coincidence with signals from the box detector we determined a resolution of 70 keV.

Higher energy sf fragments were measured in a second branch of the electronic circuit including low-gain amplifiers. Energies up to 320 MeV were measurable. A normalization of the different amplifications and an α-based calibration was performed with α particles from external sources of ^{148}Gd, ^{239}Pu, ^{241}Am, ^{244}Cm, and ^{227}Ac, which cover an energy range from 3183 to 7450 keV. The total kinetic energy (TKE) of sf events was obtained by summing the energies from the stop and the box detectors. Energy calibration of the TKE was performed with the known TKE of 195 MeV of ^{252}No [16] produced in the reaction $^{48}\mathrm{Ca} + ^{206}\mathrm{Pb}$. Pulse height deficits and energy loss in the inactive entrance windows of stop and box detectors were determined from the difference compared to the calibration using α particles. We measured a strong de-

pendence as a function of the implantation depth which was regulated by varying a number of Mylar degrader foils in front of the Si detector array. Seven different thicknesses ranging from 1 to 8 μm were used. This information was needed for the calibration of the TKE of sf events of nuclei produced in the reaction $^{30}Si + ^{238}U$ at implantation depths less deep as in the case of $^{48}Ca + ^{206}Pb$. At a reaction energy of $E_{c.m.} = 133.0$ MeV, the implantation energy relative to the data from the ^{252}No test case was so that a correction energy of 55 MeV had to be added to the energy value based on α calibration in order to get the correct TKE value.

Behind the stop detector we mounted a second Si PIPS detector for detection of protons or α particles originating from inelastic reactions with the target or the target backing, which passed SHIP as background. Behind this veto detector we mounted a clover detector consisting of four Ge crystals, each with 50 mm diameter and 70 mm length. It was used to measure coincident γ- or X-rays. With two electronic branches the energy of γ-rays was measured up to ranges of 1.8 and 8.0 MeV, respectively. Due to the high multiplicity of γ-rays emitted from the fragments during sf, γ-rays in coincidence with high-energy signals from the Si detectors are likely to occur and thus serve as a strong evidence for the occurrence of sf. In the case of sf of ^{252}No we measured in 80% of all sf events at least one coincident γ-ray, whereas from high-energy background events only 2% were accompanied by one or more signals from the clover detector.

The detection of correlated events is primarily based on the agreement of the measured positions between implanted ERs and subsequent α decays or sf. The range of position distributions of correlated events for shallow implantations, as it is the case in the reaction $^{30}Si + ^{238}U$, was determined from the implantation and decay of ^{252}No produced in the reaction $^{48}Ca + ^{206}Pb$ using a 5 μm thick Mylar degrader foil in front of the Si detector array. A position resolution of 0.4 mm (FWHM) was determined between ERs and α particles fully absorbed in the stop detector. For ERs and escaping α particles the resolution was 2.9 mm. Correlation between ERs and sf resulted in 1.2 mm position resolution.

In order to test a possible production of spontaneously fissioning nuclei in reactions with a ^{208}Pb contamination of the uranium targets, we investigated the reaction $^{30}Si + ^{208}Pb \rightarrow ^{238}Cm^*$ at beam energies of 152.4 and 158.1 MeV. SHIP was set for filtering out ERs. At 152.4 MeV, no sf was observed at a beam dose of 1.2×10^{17}. At 158.1 MeV, two sf events were detected at a beam dose of 1.7×10^{17}, corresponding to a cross-section of 180 pb. This cross-section value agrees with the one measured for sf of ^{234}Cm produced in the reaction $^{40}Ar + ^{198}Pt \rightarrow ^{238}Cm^*$ [17]. Considering a maximum ^{208}Pb contamination of 1.2×10^{-6} in the uranium targets according to the material contamination analysis, we estimated a probability of 1×10^{-4} for the observation of one sf event originating from ^{208}Pb impurities in each of our three $^{30}Si + ^{238}U$ irradiations.

Table 1. Parameters of the ^{30}Si beam used in irradiations of ^{238}U targets. E_{lab} is the energy in front of the target, the center-of-mass energy $E_{c.m.}$ and the excitation energy E^* are calculated for reaction at half thickness of the target.

E_{lab}/MeV	$E_{c.m.}$/MeV	E^*/MeV	dose/10^{18}
163.5	144.0	50.6	1.8
151.2	133.0	39.6	4.0
145.5	128.0	34.5	1.7

3 Experimental results and discussion

3.1 Produced isotopes

The irradiations at SHIP took place from April 8–May 1, 2006. We used three different beam energies which where chosen so that for reactions at half thickness of the target maximum cross-sections were expected for the evaporation of five, four, and three neutrons, respectively, according to a statistical model calculation (for details see sect. 3.2). Beam energies, resulting excitation energies of the compound nuclei and beam doses are listed in table 1.

We started our experiment using the highest beam energy. At that energy we expect the highest ER cross-section which was calculated for the emission of five neutrons. The decay properties of the produced isotope ^{263}Sg are sufficiently well known, so that an unambiguous identification is possible [18–23]. We observed four decay events which are shown in the upper row in fig. 1, chronologically ordered from 1 to 4.

Event number 1, 2, and 4 were obtained during measurement without timing detector, resulting in the higher implantation energy, whereas number 3 was obtained during a period when the timing detector was positioned in front of the Si detector array. Subsequent to the implantation, we measured within the position resolution of the detector two α decays in the case of event number 1 and 2, three α decays in the case of event number 3. Energies and half-lives agree well with the literature data for ^{263}Sg, see references given before. The large energy of 4729 keV deposited in the stop detector for the decay of ^{259}Rf in the case of event number 2 is due to the shallow angle of emission of the α particle relative to the surface of the stop detector. From the measured position in the stop detector and the location of the hit box detector segment, we obtained an emission angle between 0 and 17 degrees.

No definite conclusions can be drawn concerning the different intensity ratios of the 9.06 and 9.25 MeV α lines from the decay of ^{263}Sg in the case of direct production in a fusion reaction, [18] and this work, or by population as granddaughter in the α decay of ^{271}Ds [20–23]. Definitely, we can conclude that the two different lines originate from two different levels. The reason is that in the case of direct production of ^{263}Sg different line intensities were measured than in the case of population by α decay within the chain from ^{271}Ds. If the different α energies would originate from transitions of one level in ^{263}Sg to different final states in the daughter nucleus ^{259}Rf, then

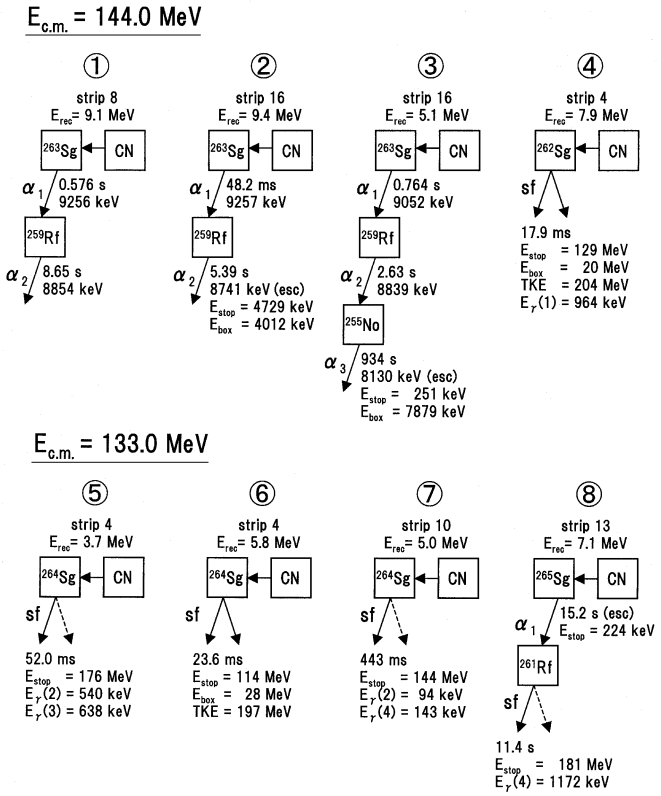

Fig. 1. Decay events obtained from the reaction $^{30}\mathrm{Si} + {}^{238}\mathrm{U} \rightarrow {}^{268}\mathrm{Sg}^{*}$ at $E_{\mathrm{c.m.}} = 144.0\,\mathrm{MeV}$ (upper row) and at $E_{\mathrm{c.m.}} = 133.0\,\mathrm{MeV}$ (lower row). In the case of α decay or spontaneous fission (sf) the energies measured in the stop and box detector are given. For sf the total kinetic energy (TKE) is given, when both fission fragments were detected. Also given are the energies of γ-rays coincident with sf measured in one or more of the four crystals of the Ge clover detector. The number in brackets gives the crystal number of the fourfold Ge clover detector.

the intensity ratio would be independent of the production mechanism.

In the discovery experiment of element 106 [18] using a relatively slow He-jet technique, from a total number of 73 counts an intensity ratio of about 9 to 1 was determined for the lines at 9.06 and 9.25 MeV [24], respectively, whereas in the decay chains of ^{271}Ds the 9.25 MeV α particles are observed almost exclusively. From a total of 36 decay chains of ^{271}Ds published in [20–23], in 22 cases the energy of the ^{263}Sg α decay is determined sufficiently well for clearly distinguishing the two different energies. Among these 22 events the majority of 20 ones has a higher energy of 9.25 MeV and only 2 have an energy of 9.06 MeV. Because the two intensity ratios are different with high statistical significance, we must assume two different levels in ^{263}Sg, although their half-lives are similar.

The mean half-life of the 20 higher-energy events is $(0.56^{+0.16}_{-0.10})$ s. This value is significantly prolonged by a statistical runaway with a lifetime of 6.0 s measured in [22]. The half-life determined from the two lower-energy events is $(0.56^{+1.02}_{-0.22})$ s. Due to the larger error bars, the latter value is in agreement with the longer half-life of (0.9 ± 0.2) s obtained from the more prominent 9.05 MeV α-rays in the He-jet experiment.

In the present experiment we observed two α decays at 9.25 MeV and one at 9.05 MeV. The measured lifetimes given in fig. 1 are in good agreement with the literature data. The intensity ratio of two to one for the energetically different α-rays indicates losses of the shorter-lived higher-energy α particles in the He-jet experiment [18]. The cross-section for the production of the three ^{263}Sg nuclei in our experiment at a beam energy of 163.5 MeV is (67^{+67}_{-37}) pb.

At this highest beam energy we observed also one sf event at a lifetime of 17.9 ms ($T_{1/2} = (12.4^{+56}_{-\ 6})$ ms), number 4 in fig. 1. No signal was detected indicating an α decay between implanted ER and sf. The sf event was in coincidence with a γ-ray at 964 keV in one of the crystals of the clover detector. Two fragments were measured in coincidence in the stop and box detector at a sum energy of 149 MeV. After correction for the pulse height deficit, 55 MeV, we obtained 204 MeV as TKE. The isotopic assignment of this sf event is difficult. Although the production yield of ^{263}Sg should be highest at this beam energy, we expect a longer sf half-life relative to the neighboring even-even isotopes due to an odd neutron hindrance factor. Half-life as well as TKE are in good agreement with the decay data of the known isotope ^{262}Sg, $T_{1/2} = 6.9$ ms, TKE = 222 MeV [25]. Slightly less agreement exists, concerning the half-life, with the isotope ^{264}Sg ($T_{1/2} = (120^{+126}_{-\ 44})$ ms, see below). The cross-section for the sf event is (22^{+51}_{-18}) pb. We tentatively assign this sf event to the isotope ^{262}Sg produced by evaporation of six neutrons. The measured TKE of 222 MeV agrees reasonably well with the value of 210 MeV obtained from the empirical Viola formula [26] for ^{262}Sg.

At the lower beam energy of 151.2 MeV, we observed four sf events. They are numbered from 5 to 8 in fig. 1. These events were measured during periods with the timing detector in front of the Si detector array resulting in the relatively low implantation energy. The events were identified as sf on the basis of the high signal amplitude, absence of signals from the timing detector and, in the case of event numbers 5, 7, and 8, coincident γ signals from the clover detector. In the case of event number 6, no coincident γ-ray was measured, however, both fission fragments were detected in the stop and box detector. In addition, this event occurred during the beam-off period. From the sum of the two fragment energies, we obtained a TKE of 197 MeV after correcting for the pulse height deficit. TKE values cannot be unambiguously determined in the other three cases, when only one signal was detected, due to the uncertainty related with the amount of lost energy. If both sf fragments are stopped in the stop detector, the correction energy differs from the value given before.

The lifetime of the sf events number 5 to 7 is similar and relatively short. We determined a half-life of $(120^{+126}_{-\ 44})$ ms. The events were produced at an excitation energy of 40 MeV, 11 MeV less than the value for the production of ^{265}Sg. At this energy we expect the high-

est yield for the evaporation of four neutrons. We assign these three sf events to the sf isotope ^{264}Sg. The TKE of 197 MeV obtained from event number 6 is in good agreement with the value of 210 MeV calculated from the Viola formula for ^{264}Sg [26].

A comparison with calculated sf half-lives reveals a shorter experimental value by about a factor of twenty. The calculated half-life given in [27] is 2.3 s. The deviation continues a trend already observed in the sf half-life of ^{262}Sg where the experimental value is about a factor of ten shorter than the calculated one, whereas agreement between experiment and theory within a factor of two exists for the isotopes ^{260}Sg and ^{258}Sg [25].

The production cross-section for the three sf events assigned to ^{264}Sg is (10^{+10}_{-6}) pb.

Preceding the fission event number 8, no α decay with $E_\alpha > 8.0$ MeV was observed up to a time range of 1000 s. However, at 11.4 s we found a 224 keV signal without signal of the timing detector, indicating an escaped α particle. An energy estimation revealed that 30% of escaping α particles have energies in the range from 200 to 300 keV. For the appearance by chance of escape-like events in the relevant detector strip and within a position window of $\Delta Y = \pm 6.0$ mm we obtained an average value of 82 s. This interval is a factor of seven larger than the time span of 11.4 s, which makes the origin of the correlation by chance unlikely.

The average frequency of ER-like events implanted within a position window of $\Delta Y = \pm 1.2$ mm is 1 per 10 s. Indeed, we measured a first ER-like event at 11.1 s before the sf event. However, due to the fact that an escaped α event occurred 11.4 s before the sf event, which has a high probability for being a true correlation, we interpret the ER-like event at 11.1 s as chance event. The first ER candidate before the sf event and escaped α particle was measured at 15.2 s before the α event. However, due to the appearance of one ER-like event every 10 s on the average, the value of 15.2 s represents only a lower limit for the lifetime.

Comparing the decay properties of event number 8 with those of reasonable candidates of seaborgium isotopes ($^{263-265}$Sg) produced in the reaction, we find good agreement with the decay of ^{265}Sg. This isotope is an α emitter with a half-life of $(7.9^{+6.4}_{-2.4})$ s (average of three events from [28] and two events from [29]). Recent investigation of ^{265}Sg and the α decay daughter ^{261}Rf produced as decay products of ^{269}Hs in the reaction $^{26}Mg + ^{248}Cm$ revealed from six measured events, firstly, a half-life of $(16.4^{+8.2}_{-4.5})$ s of ^{265}Sg and, secondly, a 100% probability for sf of the $T_{1/2} = (3.6^{+2.3}_{-1.1})$ s state in ^{261}Rf populated by α decay of ^{265}Sg [30]. Due to the good agreement of these data with our data from event number 8, we tentatively assign our event to ^{265}Sg. The production cross-section at $E_{\mathrm{c.m.}} = 133.0$ MeV is $(3.5^{+8.1}_{-2.9})$ pb.

At the lowest beam energy of 145.5 MeV no decay events were measured. We determined an upper cross-section limit of 15 pb at 68% confidence level (one event would have had a cross-section of 8.2 pb).

3.2 Discussion of the production cross-sections

Experimentally determined cross-sections of the reaction $^{30}Si + ^{238}U \rightarrow ^{268}Sg^*$ are compared with two different calculations in fig. 2. The upper part shows the fission cross-section measured at JAEA [31] by detecting single fragments. These data are used here prior to publication. The fission fragments can originate from quasifission and compound-nucleus fission, so that the cross-section represents the sum of both origins. The data are compared with the results for the capture cross-section using the coupled-channel code CCDEGEN [32] which is a modification of the code CCFULL [33]. In the calculation the static deformation of the target nucleus ^{238}U with the deformation parameters $\beta_2 = 0.275$ and $\beta_4 = 0.05$ [5,34] is taken into account. The nuclear potential was approximated by using the same parameters as in the case of the earlier studied reaction $^{16}O + ^{238}U \rightarrow ^{254}Fm^*$ [5]. Also considered was the channel coupling to the 3^- state at 0.73 MeV in ^{238}U and to the 2^+ state at 2.235 MeV in ^{30}Si. We also show in fig. 2 the results from the CCDEGEN code using the assumption of a spherical target nucleus and no coupling to excited states in projectile and target nuclei (one-dimensional model). The corresponding Coulomb barrier height is 139.7 MeV.

The coupled-channel calculation (solid curve in the upper part of fig. 2) reproduces well the experimental data points for the reaction $^{30}Si + ^{238}U$ as it was the case for the lighter system $^{16}O + ^{238}U$ [5]. However, it does not give information about the increasing amount of quasifission in the capture cross-section in the case of the heavier system. The one-dimensional model, on the other hand, which does not include detailed properties of the reaction partners is not able to describe the data below the energy $E_{\mathrm{c.m.}} = 140$ MeV, where these properties become significant.

In the lower part of fig. 2. we compare the cross-sections of the fusion evaporation channels (3n–6n) measured in this work with model calculations. Using the results of the two different models for the capture cross-section (entrance channel) as discussed above, the cooling down of the compound nucleus by evaporation of neutrons and competitive fission was approximated by the statistical model code HIVAP [35].

The measured ER cross-section for the 5n channel, ^{263}Sg, at $E_{\mathrm{c.m.}} = 144.0$ MeV agrees well with both calculations (solid curve for the coupled-channel calculation and dashed curve for the one-dimensional calculation).

At the lower energy $E_{\mathrm{c.m.}} = 133.0$ MeV the large enhancement of the 4n ER cross-section compared to the one-dimensional model confirms the validity of using the nuclear properties of projectile and target in the coupled-channel calculation. The dominating reason for the enhancement is the lowering of the Coulomb barrier height for reactions with the polar regions of the deformed ^{238}U. However, the experimental 4n cross-section (10 pb) is about a factor of 4 smaller than the calculated cross-section (40 pb), a reduction which is not observed in the capture cross-section. This indicates that at this energy about 80% of the reaction does not result in fusion but in

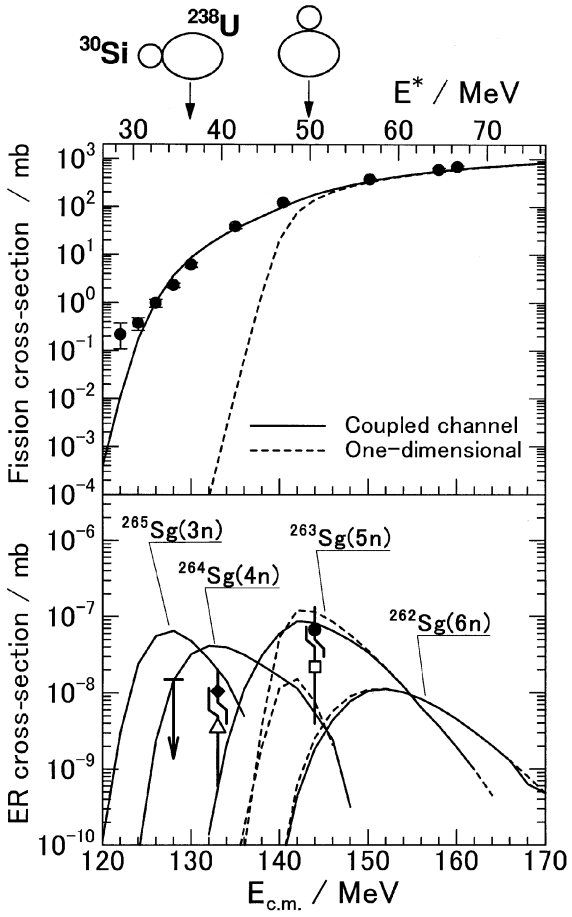

Fig. 2. Fission (upper part) and evaporation residue (ER) cross-sections (lower part) of the reaction $^{30}\mathrm{Si} + ^{238}\mathrm{U} \rightarrow ^{268}\mathrm{Sg}^*$ as a function of the center-of-mass energy $E_{\mathrm{c.m.}}$ and excitation energy E^* for reactions at half thickness of the target. In the upper part, the experimental data points, taken from [31], include quasifission and compound-nucleus fission. The data are compared with results for the fusion cross-section of a coupled-channel calculation (full line) and of a one-dimensional fusion model (dashed line, see text). The calculated ER cross-sections in the lower part were determined from the calculated fusion cross-sections using the statistical evaporation code HIVAP [35]. At $E_{\mathrm{c.m.}} = 133.0$ and 144.0 MeV three events were measured in each case for the 4n (diamond) and 5n (circle) evaporation channel, respectively, and one event in each case was tentatively assigned to the 3n (open triangle) and 6n (open square) channel, respectively. The two extreme touching configurations, polar and equatorial collisions are shown at the top of the figure. There the two arrows indicate the corresponding Coulomb barrier heights.

re-separation of the reaction partners via the quasifission channel.

Also at the lowest energy $E_{\mathrm{c.m.}} = 128.0$ MeV the measured upper limit of the cross-section of 15 pb (3n + 5n channel) is about a factor 5 less than the calculated one, indicating a strong quasifission contribution.

Finally, we compare the two extreme reactions mentioned before, namely, the very asymmetric system $^{16}\mathrm{O} + ^{238}\mathrm{U}$ [5] which has an orientation-independent fusion probability and the heaviest systems studied so far using $^{48}\mathrm{Ca}$ projectiles [3,4], with the reaction $^{30}\mathrm{Si} + ^{238}\mathrm{U}$ studied here. Obviously, the reaction $^{30}\mathrm{Si} + ^{238}\mathrm{U}$ shows an intermediate behavior. We observe a strong reduction, but still a measurable fusion cross-section at low energies, where a contact configuration can be reached only in polar collisions. No reduction of the ER cross-section was measured at energies which were higher than the Coulomb barrier for equatorial collisions, indicating the high probability of complete fusion when the interaction starts at this compact configuration.

4 Summary and conclusion

We measured evaporation residue cross-sections of the reaction $^{30}\mathrm{Si} + ^{238}\mathrm{U} \rightarrow ^{268}\mathrm{Sg}^*$. At an energy of $E_{\mathrm{c.m.}} = 133.0$ MeV which is subbarrier according to a one-dimensional fusion model, we observed four spontaneously fissioning nuclei. Three of the events have similar half-lives with an average value of $(120^{+126}_{-\ 44})$ ms. We attribute these events to the fissioning isotope $^{264}\mathrm{Sg}$.

The cross-section for the production of this isotope at this energy is $(10^{+10}_{-\ 6})$ pb. This value indicates a large underestimation of about factor 1×10^{-4} of the cross-section calculated with the one-dimensional fusion model. Compared to a coupled-channel calculation taking into account deformation of the target nucleus, the agreement is considerably better. However, in this case a fraction of 80% of the capture cross-section had to be assigned to quasifission in order to explain the measured 4n ER cross-section.

At the higher energy $E_{\mathrm{c.m.}} = 144.0$ MeV, where the projectile starts to interact with the deformed target nucleus $^{238}\mathrm{U}$ from the equatorial side, we obtained four decay chains. The decay properties of three of them are in agreement with those of the known isotope $^{263}\mathrm{Sg}$. The 5n ER cross-section is (67^{+67}_{-37}) pb. No significant reduction of the cross-section was observed at this energy in comparison to the results of the coupled-channel calculation. This supports the idea that the fusion starting from a compact configuration is advantageous in the fusion processes using deformed target nuclei.

We thank the UNILAC staff for preparation of the stable and intense $^{30}\mathrm{Si}$ beam. We are also grateful to W. Hartmann and J. Steiner of the GSI target laboratory for manufacturing the target wheels and H.G. Burkhard for taking care of the mechanical devices at SHIP. We thank K.E. Gregorich and Ch.E Düllmann for making available to us preliminary data obtained at LBNL of the same reaction as studied here, prior to our experiment. One of us (K.N.) would like to express his gratitude for kind hospitality and excellent working conditions at GSI. This work was partly supported by a Grant-in-Aid for Scientific Research of the Japan Society for the Promotion of Science.

References

1. S. Hofmann, G. Münzenberg, Rev. Mod. Phys. **72**, 733 (2000).

2. K. Morita *et al.*, J. Phys. Soc. Jpn. **73**, 1738 (2004).
3. Yu.Ts. Oganessian *et al.*, Phys. Rev. C **69**, 054607 (2004).
4. Yu.Ts. Oganessian *et al.*, Phys. Rev. C **70**, 064609 (2004).
5. K. Nishio *et al.*, Phys. Rev. Lett. **93**, 162701 (2004).
6. K.E. Gregorich, private communication (2006).
7. K. Nishio *et al.*, Phys. Rev. C **62**, 014602 (2000).
8. S. Mitsuoka *et al.*, Phys. Rev. C **62**, 054603 (2000).
9. K. Nishio *et al.*, Phys. Rev. C **63**, 044610 (2001).
10. S. Mitsuoka *et al.*, Phys. Rev. C **65**, 054608 (2002).
11. G. Münzenberg *et al.*, Nucl. Instrum. Methods **161**, 165 (1979).
12. S. Hofmann, *et al.*, Z. Phys. A **291**, 53 (1979).
13. H. Folger *et al.*, Nucl. Instrum. Methods A **362**, 64 (1995).
14. B. Lommel *et al.*, Nucl. Instrum. Methods A **480**, 16 (2002).
15. R. Mann *et al.*, GSI Scientific Report 2003, 224 (2004).
16. E.K. Hulet, Phys. At. Nucl. **57**, 1099 (1994).
17. P. Cagarda, PhD Thesis, Comenius University, Bratislava (2002).
18. A. Ghiorso *et al.*, Phys. Rev. Lett. **33**, 1490 (1974).
19. S. Hofmann, Rep. Prog. Phys. **61**, 639 (1998).
20. S. Hofmann, J. Nucl. Radiochem. Sci. **4**, R1 (2003).
21. T.N. Ginter *et al.*, Phys. Rev. C **67**, 064609 (2003).
22. K. Morita *et al.*, Eur. Phys. J. A **21**, 257 (2004).
23. C.M. Folden III *et al.*, Phys. Rev. Lett. **93**, 212702 (2004).
24. R.B. Firestone, V.S. Shirley (Editors), *Table of Isotopes*, Vols. **1** and **2**, eighth edition (John Wiley and Sons, Inc., New York, 1996).
25. S. Hofmann *et al.*, Eur. Phys. J. A **10**, 5 (2001).
26. V.E. Viola, jr., Nucl. Data A **1**, 391 (1966).
27. R. Smolanczuk *et al.*, Phys. Rev. C **52**, 1871 (1995).
28. A. Türler *et al.*, Eur. Phys. J. A **17**, 505 (2003).
29. S. Hofmann *et al.*, Eur. Phys. J. A **14**, 147 (2002).
30. J. Dvorak *et al.*, GSI Scientific Report 2004; GSI Report 2005-1, 71 (2005).
31. K. Nishio *et al.*, unpublished.
32. K. Hagino, unpublished.
33. K. Hagino, N. Rowley, A.T. Kruppa, Comput. Phys. Commun. **123**, 143 (1999).
34. D.J. Hinde *et al.*, Phys. Rev. Lett. **74**, 1295 (1995).
35. W. Reisdorf, M. Schädel, Z. Phys. A **343**, 47 (1992).